

Studies of selected voids. Surface photometry of faint galaxies in the direction of 1600+18 in Hercules void.

Georgi Petrov¹

Institute of astronomy and NAO, Bulgarian Academy of Sciences,
72 Tsarigradsko chaussee, 1784 Sofia, Bulgaria.
petrov@astro.bas.bg

(Submitted on 18.05.2013; Accepted on 21.06.2013)

Abstract. Surface photometry, coordinates, magnitudes $m(B)$, diameters, position angles and some morphological parameters are presented for ca. 1850 faint galaxies in a field of one square degree centered at 1600+18 (1950) (Hercules void). The distribution of the magnitudes of the galaxies in this direction is compared with "Log Normal" and "Gauss" ones and with similar results from SDDS studies of galaxies. Some candidates for primeval galaxies – 38 large Low surface brightness galaxies were detected in the direction of the void. Major axes luminosity profiles are analyzed. Comparison between two different methods for automatic selection and classification – a new package, based on MIDAS INVENTORY and SExtractor packages have been made.

Key words: astronomy: Voids, Galaxies, Astrometry, Photometry, Morphology

Introduction

The scientific results shown in this paper are part of a collaborative project between the Institute of Astronomy, Bulgarian Academy of Sciences and Max Planck Institute of Astronomy, Heidelberg, Germany. The project was devoted to investigation of some known voids. For details further information concerning voids see Oort (1983) and Rood (1988).

Because of large quantity of data after full surface photometry procedure these results still have not been published. Partially some results co. voids were reported during the Balkan Astronomical Meeting'2004 (Petrov et al., 2005), Fifth Bulgarian-Serbian Conference (Petrov et al., 2007) and the International astronomical conference "NAO Rozhen - 30 years eyes to the sky", Smolyan, September'2011 (Petrov, 2012).

In section 1 observations and reductions are described. In section 2 main INVENTORY results are presented. Comparison between two methods for automated selection and classification is presented. In section 3 the morphological parameters of the galaxies are studied and some steps toward the understanding the nature of primeval galaxies are marked. In section 4 some SeXtractor results are discussed. Section 5 contains conclusions and discussion.

1. Observations and reductions

During the nights of 27 and 28 june 1991 two plates with coordinates (2000.0) of the center – No.1830 RA: 16h 01m 58s and DEC: +17d 57' 30" and No.1831 RA: 16h 02m 15s and DEC: +17d 51' 43" were taken as a part of collaborative project between MPIA, Heidelberg, Germany and IA of BAS (Petrov et al., 1993). The Ritchie camera of the 2-m RCC telescope at National Astronomical Observatory, Rozhen - Bulgaria was utilized. ORWO plate ZU21 30x30 sq. cm and Schott filter GG 385 were combined to realize the standard B-system.

The exposition time for the two plates was 180 minutes, enough to detect objects fainter than 21 mag. Neutral wedge was exposed for 40 minutes on each plate after the main exposure. The seeing was very good – ca.1" - 1.5". The unvignetted field is ca. 50 sqr. minutes for each plate and common unvignetted field is ca. 1x1 sqr.deg.

Two sets of CCD frames in B and R were taken with 1024 x 1024 sqr. px Photometrics camera, attached to the prime focus on the 2_m RCC telescope during the night of 28.07.2003. M92 standard fields (Cristian et al., 1985) were taken twice during the same night.

In our earlier work (Petrov et al., 1999) coordinates of 1745 galaxies, all that were detected visually on the two plates, were measured on an GLAREX machine in MPIA Heidelberg. SAO standard stars taken with OVERLAY program developed by MPIA, were used as astrometric standards. Another program – AMETRY was used to convert the rectangular coordinates to equatorial ones. Third order polynomial was used to determine the coefficient of transformation of the coordinates. After the procedure of visual inspection of glass copy of POSS we got 225 galaxies in the same field.

In the same time, 207 galaxies, Radio sources, Ir Sources and X_ray Sources were catalogued in NED till the end of 2003 in the same 1 x 1 sqr.deg. field. Now after SDSS a lot of objects were found in the same region – see, e.g NED search with "near position" option.

In the second stage of this study the two plates were scanned in the former Astronomical Institute, University of Muenster on PDS 2020 GMplus scanning machine with 25x25 mkm square slit and 20 mkm step, getting 14400 x 14400 sqr.px with scale 0."25/px and seeing of 1" covering 4 px. (see Schuecker et al., 1989 and citation herein).

The linearization of the images was performed with a photometer wedge super exposed on the plates and the program package INTENAIP from the AIP context added from dr. G. Richter, Potsdam to the ESO MIDAS package.

All the reduction after uses d-r Kniazev's realization of the AIP context of ESO-MIDAS package (Kniazev et al., 2003) and standard INVENTORY package.

2. INVENTORY results

Automatic procedure for finding objects above the given background (Kniazev et al., 2003) was used. The program finds galaxies and stars. The new program package created for the purposes of discovering Low Surface Brightness Galaxies from the Sloan Digital Sky Survey is based on the Kitt Peak International Spectral Survey (for **KISS** see Salzer et al. 2000) reduction package (Kniazev et al. 1997, 1998) and some programs from the Astrophysical Institute of Potsdam (**AIP**) package in MIDAS (Lorenz et al., 1993; Kniazev, 1997) for adaptive filtering and topological operations with masks.

These programs have been recompiled for our purpose – to discover and make photometry and astrometry of all galaxies in the direction of some voids. The basic steps are:

- Search for all objects in the field and construct the main table
- Convert X,Y in RA,DEC

- First separation Stars/Galaxies
- Photometry of selected objects
- Visual inspection of all selected objects and separation of close pairs
- Deleting all multiple identified objects
- Determining magnitudes and surface brightness in 25_isophote
- Comparison with other galaxy number counts – e.g. with SDSS

As a result of three independent interactive visual selection and confirmation we found 1171 galaxies on plate No.1830 and 1229 on plate No.1831 with the limiting B_magnitude of 20.72 and 21.85 respectively. Figure 1 presents distribution of detected galaxies in RA_DEC plane.

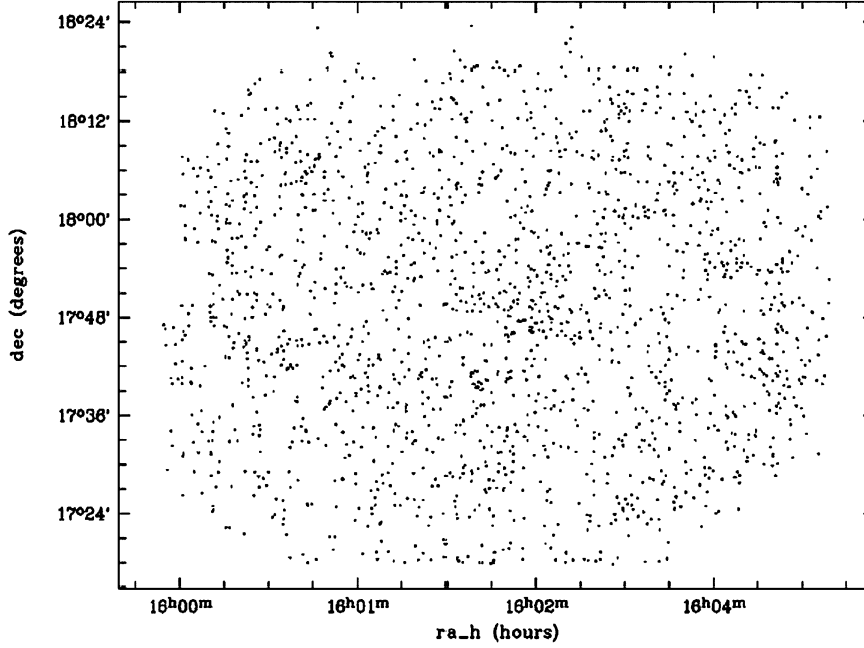


Fig. 1. Distribution of selected galaxies in the region of Hercules void

The main MIDAS Table 1 contains all information about the detected galaxies: accurate positions X_{cent} , Y_{cent} , major axes $Large_D$, axis ratio AX_RA , position angle Pos_A , coordinates RA , DEC (2000), total flux B_{fl} , effective radius R_{eff} , integrated magnitudes B_t and B_{msk} with its uncertainties, effective radii with 50% and 90% of the luminosity – $R50_B$ and $R90_B$ (in arcsec), effective surface brightness SBB_{50} and SBB_{90} in mag/sqr.arcs, concentration indices C , composite $SDSS_like_NAME$ and radii for determining the magnitudes to 25_isophote with their uncertainties (in arcsec). The table containing large quantity of data has been constructed as two_parts –

Tabl.1 and Tabl.2. Here is some extraction from the data for illustration purposes only. The table could be accessed in electronic form from the site of the Bulgarian Astronomical Journal www.astro.bas.bg/AIJ/, volume 19, under the names "Studies of gelected voids. Table 1" and "Studies of gelected voids. Table 2".

Table 1. V16full-part1 – extractions

Seq	D	ratio	PA	ra	dec	B_msk	eB_msk	RB_ef	SBB_ef	B_t	RB_50	SBB_50
1	10.77	0.789	64.5	239.9728	17.7849	19.83	0.289	1.88	23.41	19.82	2.34	23.25
2	28.42	0.545	-21.1	239.9759	17.7767	18.60	0.184	3.15	22.29	18.59	4.42	23.58
3	17.82	0.984	64.6	239.9766	17.7437	19.06	0.216	2.71	22.98	19.05	2.84	22.90
4	13.87	0.857	54.4	239.9790	17.4893	19.20	0.224	2.19	22.58	19.20	2.10	22.23
5	26.29	0.350	-22.1	239.9850	17.6762	20.10	0.324	2.48	22.82	20.05	4.27	25.16
6	12.00	0.928	-59.5	239.9851	17.5688	20.03	0.308	2.08	22.56	20.04	1.93	22.97
1847	18.13	0.868	84.5	241.0880	17.6810	18.87	0.262	2.03	22.39	18.87	2.00	22.37
1848	22.05	0.808	83.4	241.0909	17.7620	18.62	0.236	1.85	21.71	18.61	1.29	21.16
1849	63.42	0.306	-71.9	241.0912	18.1387	16.92	0.114	4.05	21.90	16.92	5.83	22.74
1850	27.16	0.929	-14.9	241.0929	18.0259	17.84	0.171	3.18	22.17	17.84	2.97	22.20
1851	19.41	0.947	28.2	241.0950	17.8298	18.95	0.273	1.95	21.95	18.95	1.02	21.00
1852	35.43	0.821	84.8	241.0961	17.8785	15.90	0.073	3.35	20.50	15.90	3.26	20.46

Table 2. V16full-part2 – extractions

Seq	RB_90	SBB_90	C	RA'2000	DEC'2000	SDSS_like_NAME	RB_25	B_25	eB_25
1	4.20	24.17	1.791	15:59:53.52	17:47:05.64	J155953+174705	3.67	20.34	0.32
2	7.32	24.27	1.657	15:59:54.24	17:46:36.12	J155954+174636	7.65	18.80	0.18
3	4.91	23.76	1.728	15:59:54.48	17:44:37.32	J155954+174437	5.64	19.22	0.21
4	4.98	23.94	2.375	15:59:54.96	17:29:21.48	J155954+172921	4.99	19.45	0.23
5	6.92	25.67	1.620	15:59:56.40	17:40:34.32	J155956+174034	3.43	21.24	0.43
6	4.05	24.31	2.101	15:59:56.40	17:34:05.52	J155956+173405	4.08	20.32	0.32
1847	5.65	23.99	2.874	16:04:21.12	17:40:51.60	J160421+174051	4.46	19.11	0.29
1848	4.23	23.10	3.687	16:04:21.84	17:45:43.20	J160421+174543	3.61	18.78	0.25
1849	14.28	24.05	2.441	16:04:21.84	18:08:19.32	J160421+180819	11.96	17.14	0.13
1850	8.06	23.73	2.832	16:04:22.32	18:01:33.24	J160422+180133	7.03	18.05	0.19
1851	5.85	24.15	7.743	16:04:22.80	17:49:47.28	J160422+174947	2.23	19.41	0.33
1852	9.37	22.11	3.168	16:04:23.04	17:52:42.60	J160423+175242	11.97	15.91	0.07

2.1. Detection

After a number of tests, at the beginning we use the combination of two filters that work one after the other with the same window size of 27 pixels – a smooth-and-clip (SAC) filter (Shergin et al., 1996) and the fast median smoothing algorithm with circular window, implemented into MIDAS by Shergin (1997). We use simple thresholding to detect galaxies with large angular sizes, and we divide this procedure into two separate iterations: 1) detection

of objects above the 3-sigma noise level on the unsmoothed images and 2) additional detection of objects above the 3-sigma noise level on the smoothed images.

Mask frames are generated during each step. For illustration, two our test galaxies with overplotted mask borders are shown in Fig.2.

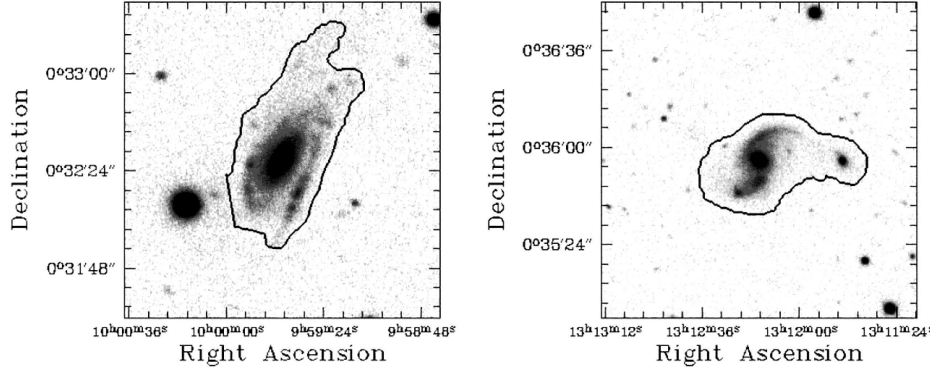


Fig. 2. Two test galaxies with overplotted mask borders.

2.2. Integrated photometry

After that the apparent flux is measured inside the same mask for background subtracted images. The instrumental flux is transformed into the apparent magnitude in the standard photometric system. For calibration we used the NED magnitudes for bright galaxies in our field.

A code for fitting the sky background from the AIP package for adaptive filtering is used, which constructs the background within the masked regions. This algorithm iteratively fills the background inside the mask by interpolating the background from the regions outside the mask (Lorenz et al. 1993; Kniazev 1997) and it is used twice: 1) to subtract any contaminating sources like foreground stars or background galaxies and 2) to fit and subtract the sky background.

2.3. Creation of surface brightness profiles

The software generates SBP by measuring magnitudes in circular apertures. As the analysis in Bremnes et al. (1999) showed, good agreement exists between an elliptical fit and circular aperture photometry. Our module is capable of measuring SBPs with any constant step size. After a SBP is created, the effective radius $R_{\text{eff_B}}$, the effective surface brightness SBB_{eff} , the radius of the region containing 90% of the integrated ($R_{\text{B_90}}$), and the concentration index $C=R_{\text{B_90}}/R_{\text{B_eff}}$ are calculated. We also use set of programs from the

AIP package to calculate the following parameters: the PA of the major axis for each filter, the axis ratio b/a , effective surface brightnesses SBB_{eff} , and effective radii RB_{eff} . All these additional parameters are calculated using the multilevel mask approach (Kniazev 1997), in which each region of intensities of the studied object is labeled with a different mask. Figure 3 and Fig. 4 present distribution of galaxies acc. to their magnitudes. The slope of the fit on Fig. 4 is 0.6.

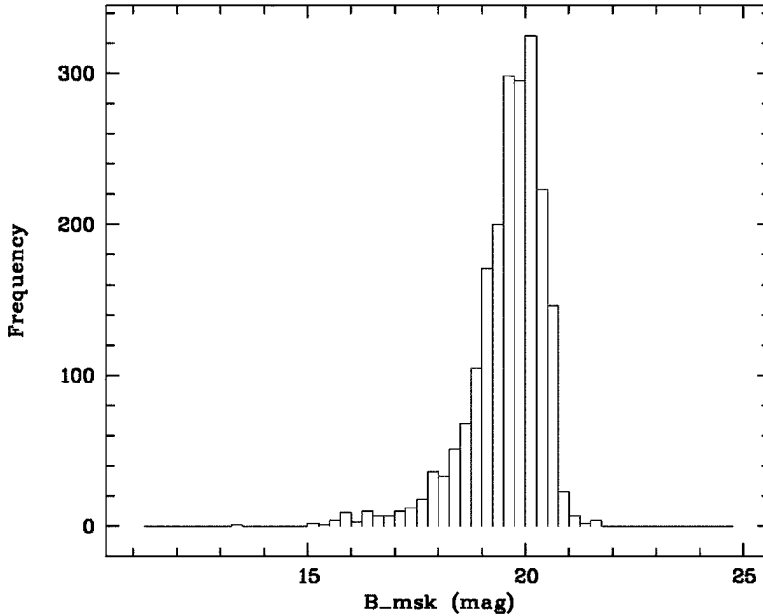


Fig. 3. Histogram of galaxies distribution acc. to their magnitudes.

2.4. Rejection of false detections

The primary selection algorithm identifies all sufficiently large objects and calculates their model-independent parameters. Thereafter we clean the list of false detections. Additionally we checked visually all the rejected objects. Since our programs are very simple and, by design, are looking for extended objects, they cannot recognize all possible blends and other complicated cases (ghosts, parts of halos around bright stars) if these have photometric parameters close to normal galaxies. Such cases thus cannot be rejected by our module automatically either. Therefore, during the second step we interactively checked all remaining candidates by eye to identify such objects.

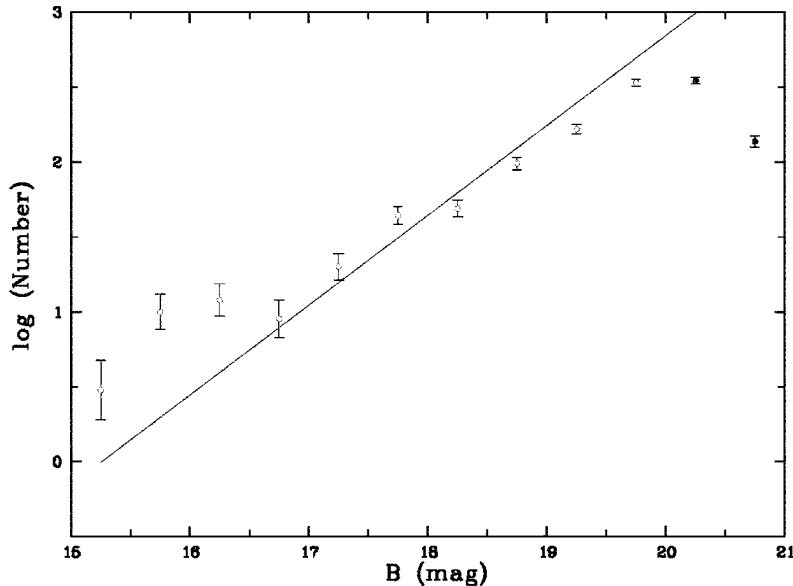


Fig. 4. Fitting of the magnitudes distribution of galaxies

3. Morphological types and concentration index

The photometric programs calculate a number of global morphological parameters for every galaxy. Some of these may be useful for morphological galaxy classifications (see earlier discussions by, e.g., Kent (1985); Kodaira et al. (1986); Fioc & Rocca-Volmerange (1999); Shimasaku et al. (2001); Strateva et al. (2001)). A particularly useful parameter is the concentration index (C hereafter), defined as the ratio of the radii containing 90% and 50% of a galaxy's light. For the classical de Vaucouleur's profile, C is ~ 5.5 , and for pure exponential disks, $C \sim 2-3$. These values are valid for the idealized seeing-free case, which we are approximating due to the limiting angular size of PSF that we impose in this work. Figure 5 and Fig. 6 present dependences of effective Surface Brightness and effective radius at 25.0 isophote from concentration index.

4. Giant LSB galaxies

An interesting aspect of this pilot study is the identification of a substantial number of luminous distant galaxies with considerable bulge and/or bar components. The underlying disks are low-surface-brightness disks with disk scale lengths in the range of ca. 7.5 to 13 kpc. These galaxies fall into the category of the so-called "giant LSB galaxies", or "cousins" of Malin 1 (Bothun et al.,

1987). On the Fig. 5 and Fig. 6 dependences of Surface Brightness and effective radius at 25.0 isophote from concentration index – R_{90_B}/R_{50_B} -ratio are presented. Here R_{90_B} and R_{50_B} are the radii containing 90% and 50% of the energy respectively.

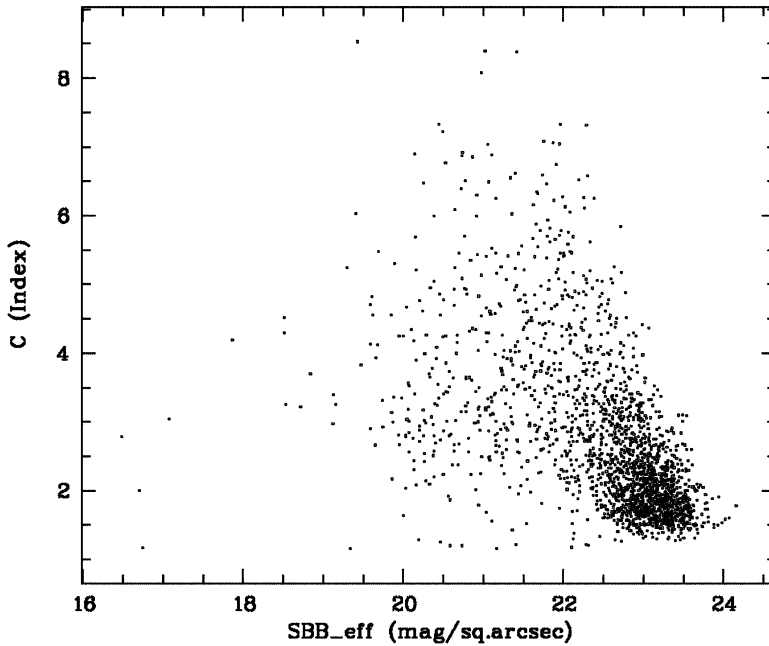


Fig. 5. Dependences of Surface Brightness at 25.0 isophote from concentration index – R_{90_B}/R_{50_B} -ratio.

The properties of giant LSB galaxies are summarized in the paper by Sprayberry et al. (1995). Currently, only few galaxies of this type are known. Turner et al. (1993), studying A3574 cluster found a significant number of large LSBG among their list with 300 objects. Kniazev et al., 2003 added a list of ten giant LSB galaxy candidates. As Bothun et al. (1997) emphasize, giant LSB galaxies are quite enigmatic from the point of view that they normally formed their spheroidal component, but no conspicuous stellar disk ever formed around their bulge. Fig.7 and Fig.8 present dependence of Surface brightness from Integrated magnitude and major diameters of galaxies. Some LSBG could be selected here – bright galaxies with B_mag ca. 15.5–18 or such ones with large - > 40 arcsec diameters and $SB > 22$ mag/sqr.sec – we select 38 large LSBG. Recently both LSBG in SDSS has been studied very actively – see e.g. Galaz et al. (2011).

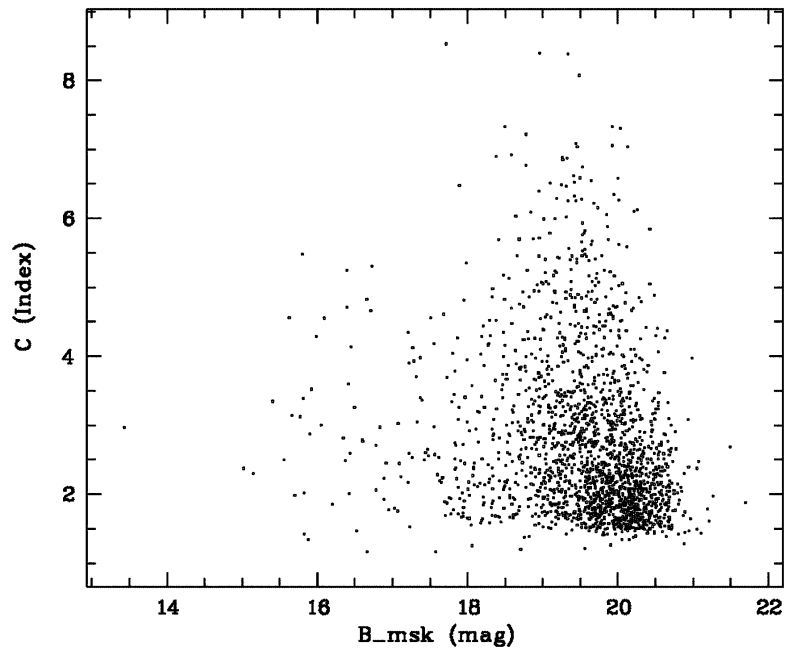


Fig. 6. Dependences of integrated magnitude from concentration index – R90_B/R50_B-ratio.

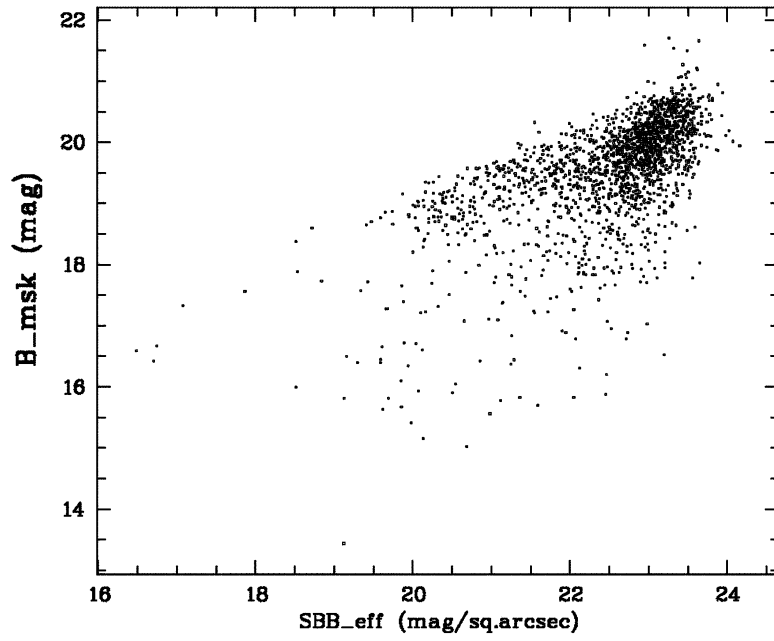


Fig. 7. Dependence of Surface brightness from Integrated magnitude of the galaxies.

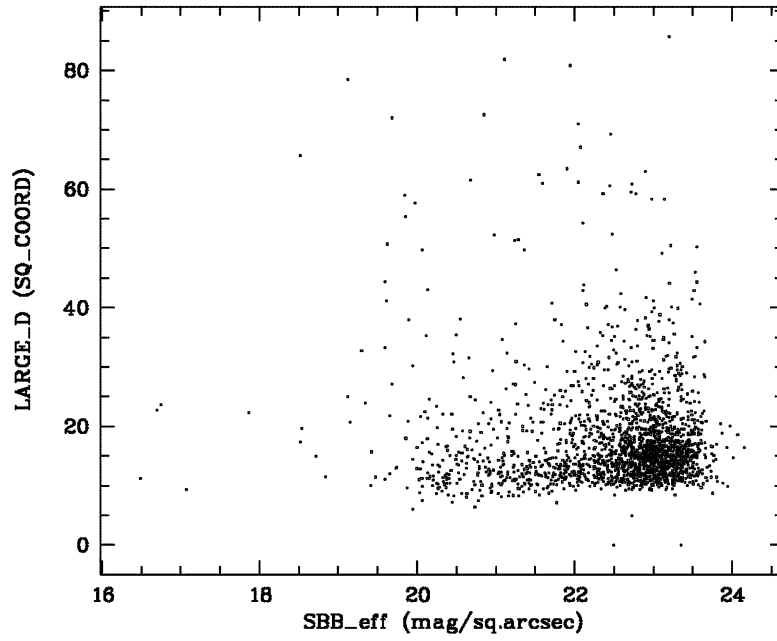


Fig. 8. Dependence of Surface brightness from the major diameters of the galaxies.

5. Results using SExtractor

Bertin's (1996) SExtractor give us the same possibilities – to find, classified as Stars or Galaxies, make aperture and isophotal photometry, astrometry and evaluate some parameters as ellipticity and elongation of the objects in question. Tuning the program correctly is the most important thing to get appropriate results. For details see Holwerda (2003). When applied to our plates we identified 3412 common objects.

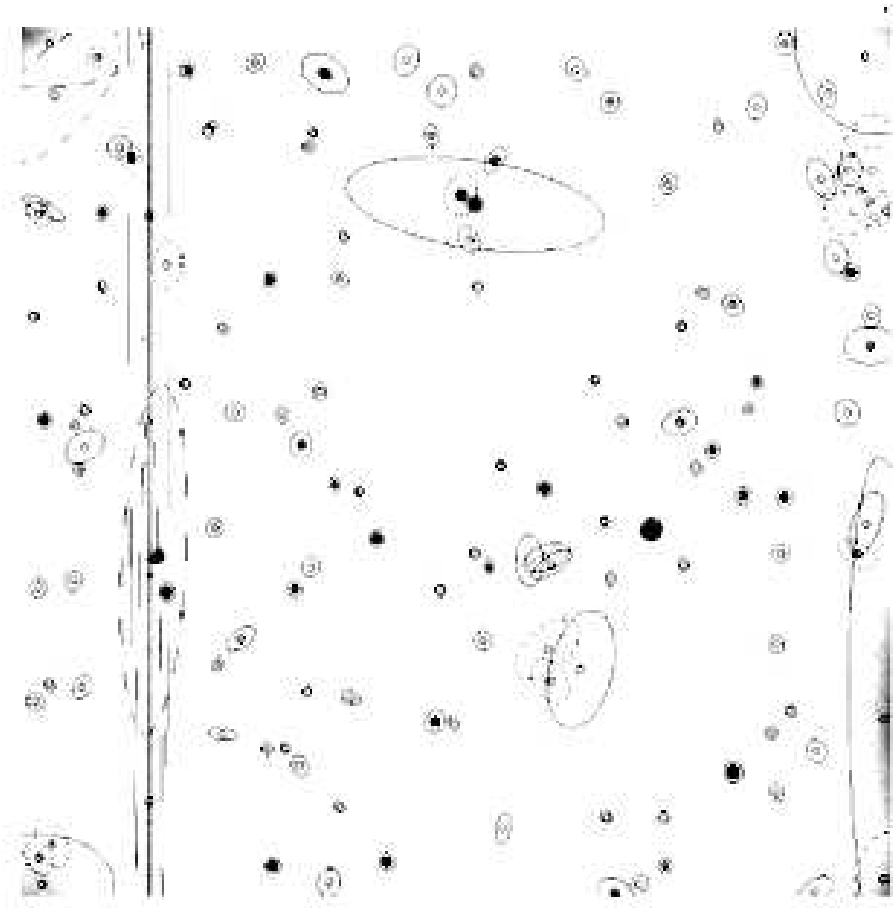


Fig. 9. CCD frame, taken on the 2_m RCC telescope of NAO. SExtractor's ellipses for each galaxy found are shown.

As it is known, automatic stars-galaxies selection is quite inefficient. We define to search all the objects with 30 pixels and above. An illustration of the isophotal photometry is presented on the Fig. 9, where 10 CCD R_frame,

taken on the 2_m RCC telescope of NAO were aligned and averaged and the photometry in the appropriate ellipses was done. SExtractor's ellipses for Mag_auto with 8 arcsec apertures are shown. Brightest "stars" here probably is galaxy – see fig. 10 below for details.

Following is a comparison between the results from search procedures with Kniazev's package and Bertin's SExtractor package – Tabl. 3.

Table 3. Comparison between the results from search procedures with Kniazev's package and Bertin's SExtractor package

Plate No.	Akn_All	Akn_Gal	Vis_gal	SE_all	SE_Akn_comm
1830	3613	1445	-	3953	-
1831	5782	1261	1665	3412	1175

6. Results

Table 4 below presents a selection of objects after execution of SExtractor (Bertin, 1996) find procedure. Here, for example, only 10 from all the 95 objects have been presented. The full Table 4 in PDF format could be reached in electronic form as *v16full-tabl4.pdf*, which can be found at the site of the Bulgarian Astronomical Journal www.astro.bas.bg/AIJ/, volume 19.

Table 4. Selection of objects after SExtractor's find procedure.

Iden	m_iso	m_ap6	m_ap8	m_ap12	m_auto	r_kron	mu_max	xcen	ycen	d_larg	elong	ellipt
19	19.031	20.082	19.656	19.167	18.738	4.550	20.757	16.94	907.33	3.52	1.34	0.25
71	21.308	21.948	21.372	20.736	19.588	7.430	22.582	17.43	202.89	2.37	1.38	0.28
82	20.918	21.978	21.479	20.724	18.841	8.710	22.473	21.48	195.52	4.79	3.78	0.74
45	16.679	17.064	16.819	16.689	16.679	3.500	17.486	23.02	428.16	2.45	1.19	0.16
70	21.205	22.031	21.485	20.768	18.849	8.710	22.646	23.74	212.91	3.88	2.43	0.59
52	18.057	19.866	19.380	18.796	17.684	5.490	20.665	927.89	347.23	6.00	1.42	0.30
79	19.775	21.625	21.141	20.471	17.684	8.110	22.170	928.86	190.43	6.84	2.20	0.55
55	21.145	21.491	21.113	20.748	20.353	6.370	22.162	929.85	314.32	2.08	1.37	0.27
81	19.218	21.666	21.023	20.206	17.075	8.430	22.071	930.30	155.59	8.18	1.96	0.49
77	21.012	22.009	21.410	20.628	19.076	8.170	22.556	945.08	199.01	2.71	1.18	0.15

Conclusions

There follow the main results and conclusions:

- Plates centered of the void 1600 +18 (1950) on the 2-m RCC telescope at NAO Rozhen, Bulgaria, with exposure 150 min and very good seeing, is received.
- More than 1850 galaxies are selected on these plates and their coordinates are measured and presented in the files described inside this paper.

- Ring aperture and isophotal photometry for all of them is performed. Magnitudes and surface brightness are presented.
- Histograms that show distribution of magnitudes and diameters by numbers of galaxies are presented.
- The presented data give us some possibility for studying LSBG population, but spectroscopic data are needed for the final conclusions or the appropriate cluster analysis of data.
- 38 large LSBG - i.e such ones with > 40 arcsec diameters and $SB > 22$ mag/sqr.sec have been found.

In the Fig.10 the object is probably a bright galaxy with star like nucleus, however classified as star in GSC - 0150700373, is presented. For comparison - see the isophotes of the star near the position (570, 505) on the frame below. The coordinate of the object are RA(2000): 16h 02m 03.41s, DEC(2000): +17d 51' 36.46".

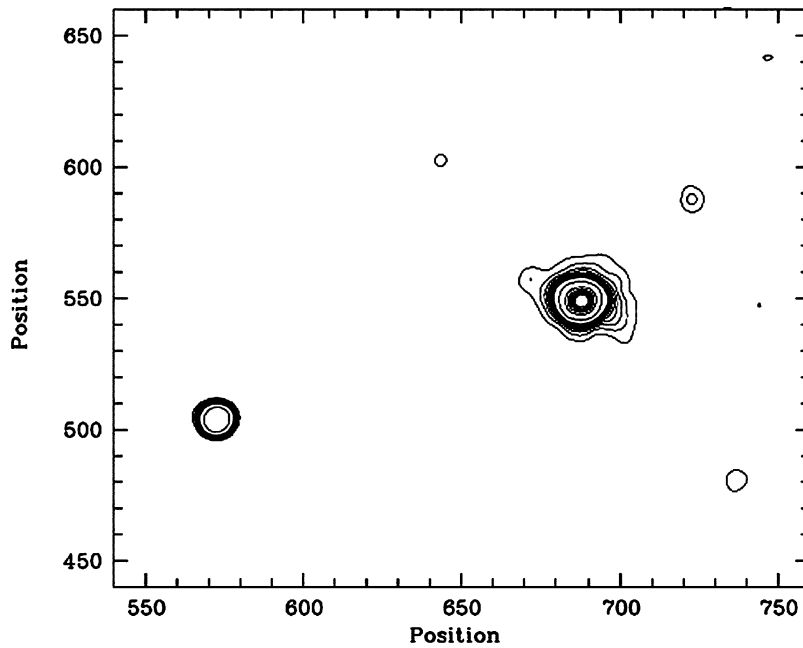


Fig. 10. The brightest star GSC 0150700373 at (690,550), $m_R = 13.8$ mag with its unusual envelop. Probably galaxy with starlike nucleus.

Acknowledgments

G.P. acknowledge financial support and hospitality of both DFG and MPIA .

This research partially has made use of the NASA/IPAC Extragalactic Database (NED) which is operated by the Jet Propulsion Laboratory, California Institute of Technology, under contract with the National Aeronautics and Space Administration.

References

- Bothun G., Impey C. & McGaugh S., 1997, *PASP*, **109**, p.745
 Bremnes, T., Binggeli, B. & Prugniel, P. 1999, *A&AS*, **137**, p.337
 Christian C.A., Adams M., Barnes J.V., Butcher H., Hayes D.S., Mould J.R., and Siegel M., 1985, *PASP*, **97**, p.363
 de Vaucouleurs G., de Vaucouleurs A., Corwin H. G. jr., Buta R. J., Paturel G. & Fouque P., 1991, *Third Reference Catalogue of Bright Galaxies*, Springer Verlag.
 de Vaucouleurs G., de Vaucouleurs A., Corwin H.G., Buta R., Paturel G. & Fouque P. 1991, *Third Reference Catalog of Bright Galaxies (New York: Springer-Verlag)*
 Fioc M. & Rocca-Volmerange B. 1999, *A&A*, **351**, p.869
 Galaz G., Herrera-Campus R., Garcia-Lambas D. & Paddila N., 2011, *ApJ*, **728**, No.2, p.74
 Holwerda B.W., 2003, "Source Extractor for Dummies".
 Huchra J. P., 1993, *GFA redshift survey catalogue*
 Kniazev A.Y., Grebel E.K., Pustilnik S.A., Pramskij A.G., Kniazeva T.F., Prada F. & Harbeck D., 2003, *AJ*, **127**, p.704
 Kniazev, A.Y. 1997, *Ph.D. Thesis, Special Astrophys. Obs., Nizhnij Arkhyz* (<http://precise.sao.ru>)
 Kniazev A.Y., Salzer J., Lipovetsky V.A., et al. 1996, in *IAU Symp. 179, New Horizons from Multi-Wavelength Sky Surveys*, Eds. B.J.McLean, D.A. Golombek, J.J.E. Hayes & H.E. Payne (Dordrecht: Kluwer), p.302
 Kniazev A.Y., Salzer J., Lipovetsky V.A., et al., 1997, *Newsletter of the Working Group on Wide Field Imaging, IAU Commission 9*, **9**, p.5
 Kodaira K., Watanabe M. & Okamura S., 1986, *ApJS*, **62**, p.703
 Lorenz H., Richter G.M. Capaccioli, M. & Longo G., 1993, *A&A*, **277**, p.321
 Oort J., 1983, *A&A Rev.*, **21**, p.373
 Petrov G., 2012, *Bulg. Astron.J Suppl.*, **1**.
 Petrov G., Fried J. & Kniazev A., 2007, *Bulg.J.Phys.*, **34**(2), p.70
 Petrov G., Kniazerv A. & Freid J., 2005, *Aerospace Research*, **20**, p.120
 Petrov G., Kovachev B. & Strigatchev A., 1993, *Astron.Ges. Abstr.Ser.*, **No.9**, p.46
 Petrov G., Strigachev A., Mihov B. & Petrov I., 1999, *C.r.BAS*, **52**, No.1-2, p.5
 Richter G.M., 1978, *Astronomische Nachrichten*, **299**, p.331
 Rood H. J., 1988, *A&A Rev.***26**, p.631
 Salzer J.J., Gronwall C., Lipovetsky V.A., Kniazev A., Moody J.W., et al. 2000, *AJ*, **120**, p.80
 Schuecker et al.,1989, *Reviews in modern astronomy*, **2**, p.109
 Shane C. D., 1975, In: *Galaxies and the Universe*. Eds: A.Sandage, M. Sandage and J. Kristian, p.647-663, Univ. of Chicago press.
 Shergin V.S., 1997, *private communication*
 Shergin V.S., Kniazev A.Yu. & Lipovetsky V.A., 1996, *Astronomische Nachrichten*, **317**, p.95
 Shimasaku K., Fukugita M., Doi M. et al. 2001, *AJ*, **122**, p.1238
 Sprayberry D., Impey C.D., Bothun G.D. & Irwin M.J., 1995, *AJ*, **109**, p.558
 Strateva I., Ivezić Z., Knapp G.R. et al. 2001, *AJ*, **122**, p.1861
 Turner J., Phillips S., Davies J. & Disney M., 1993, *MNRAS*, **261**, p.39